Electronic Supplementary Information

Layered MoS_2 defect-driven in-situ synthesis of plasmonic gold nanocrystals visualizes the planar size and interfacial diversity

Bang Lin Li, [a,*] *Hao Lin Zou,* [a] *Hong Qun Luo,*[a] *David Tai Leong,*[b,*] *and Nian Bing Li*[a,*]

[a] School of Chemistry and Chemical Engineering, Southwest University, Chongqing 400715, P. R. China.

[b] Department of Chemical and Biomolecular Engineering, National University of Singapore, Singapore 117585, Singapore.

*Correspondence and requests for materials should be addressed to B. L. Li (chemlibl@swu.edu.cn), D. T. Leong (cheltwd@nus.edu.sg) and N. B. Li (linb@swu.edu.cn).

1. **Materials.** Molybdenum disulfide (MoS_2 crystalline powder, < 2 μm, 99%) was obtained from Sigma-Aldrich Co. (USA). Sodium cholate (98%), chloroauric acid hydrated ($HAuCl_4 \cdot 4H_2O$), L-cysteine (Cys), and glutathione (GSH) were obtained from Aladdin Chemistry Co. Ltd. (Shanghai, China). Bovine serum albumin (BSA) was purchased from BBI Life Science (Shanghai, China). Other chemicals were of analytical reagent grade and used without further purification. Ultrapure water (18.2 MΩ cm) was utilized throughout the whole experiment.

2. **Experimental Instrumentations.** A KQ-400B ultrasonic bath (400 W, Kunshan Ultrasonic Instruments Co., Ltd., China) was adopted for the liquid-phase exfoliation of MoS_2 crystals. The optical absorption spectra were recorded on a UV-2450 UV-vis spectrophotomer (Shimadzu, Japan). The processing growth of Au nanostructures on layered MoS_2 was observed using TEM. X-ray photoelectron spectra (XPS) results were analyzed using an ESCALAB 250Xi X-ray photoelectron spectroscope (Thermo Electron, USA). Raman spectra were recorded on a confocal laser Raman spectrometer (Renishaw, UK) with an excitation wavelength of 532 nm. Size fractionations were conducted using a TGL-16M high-speed refrigerated centrifuge (Xiangyi, China). Morphological characterization of nanostructures and energy dispersive X-ray spectroscope (EDS) element mapping were conducted using a TecnaiG2 T20 UTWIN (FEI, USA) transmission electron microscope (TEM). Fourier Transform infrared (FTIR) spectra were performed for characterizations of MoS_2 interfacial modification (Bruker, Germany). Inductively coupled plasma-atomic emission spectra (ICP-AES) were employed for the quantitative analysis of Mo species concentrations.

3. **Liquid-Exfoliated and Differential-Rate Centrifugation Strategies.** Briefly, a portion of 100.0 mL mixed aqueous dispersion, containing 5.0 $mg \cdot mL^{-1}$ MoS_2 powders and 1.5 $mg \cdot mL^{-1}$ sodium cholate, was treated with sonication (25℃, 20 h).[S1-S3] The resultant dispersion was centrifuged (1500 rpm, 30 min) and yellow-green supernatant was collected to remove un-exfoliated bulk crystals. In order to achieve size fractionation, the separated supernatant was centrifuged at 2000 rpm for further 30 min, and subsequently, the sediments of MoS_2 samples (2k-MoS_2) and yellow-green supernatant (2k-S) were isolated, respectively.[S4] The sediments of 2k-MoS_2 were re-dispersed in aqueous solutions with sonication treatments for stocking solutions of 2k-MoS_2. Afterwards, the dispersed

solution of 2k-S was further treated with higher-speed centrifugation (4000 rpm, 30 min). Then, the sediments (4k-MoS_2) and supernatant (4k-S) were separated for the collection of MoS_2 samples and dispersed solutions, respectively. Similar to the above treated strategy, the dispersed solution was further utilized for the presentation of additional MoS_2 samples, including 6k-MoS_2, 8k-MoS_2, and 10k-MoS_2.[S4]

4. **Reactions Between MoS_2 and Chloroauric Acid.** Firstly, a portion of 9.0 mL chloroauric acid solution was pre-heated in a water bath (40 °C) and kept stirred (300 rpm) for 30 min. Subsequently, a portion of 1.0 mL MoS_2 aqueous dispersion was added to the treated chloroauric acid solution, whereas the reaction occurred immediately and terminated after 30 min. The resultant solution was taken out from the water bath for naturally cooling. As-obtained colorful dispersions were treated with centrifugation (10 000 rpm, 20 min), and sediments were further re-dispersed in a certain volume of ultrapure water for purification of hybrids. The products of Au/MoS_2 nanoarchitectures stocking solutions were stored at 4 °C for further experiments.

5. **The Freezing Treatments Collecting Intermediate States of Reactions.** After MoS_2 was incubated with $HAuCl_4$ with diverse reaction times, the intermediate states were collected and analyzed using the freezing strategies. Firstly, the aqueous mixture solutions (1.5 mL) were frozen via rapidly transferring it into the liquid nitrogen for 10 min. Next, the stored tubes were taken out for centrifugation (4 °C, 30 min). Significantly, sediments were collected and subsequently re-dispersed into the ultrapure water for characterization.

6. **Incubation of LE MoS_2 with Modifiers.** LE MoS_2 nanosheets were functionalized with extra modifiers (cysteine: Cys; glutathione: GSH; 2-mercapto-ethylamine: MEA; bovine serum albumin: BSA; fetal bovine serum: FBS) on their surfaces.[S5-S7] A portion of 0.9 mL MoS_2 dispersion (1.0 mM) was mixed with 0.1 mL 5.0 mM thiol small molecules or micromolecules, and the mixture solution was subsequently incubated for 12 h at 4 °C. After that, the mixture was centrifugated at 10000 rpm for 25 min, and sediments were collected. The sediments were re-dispersed in ultrapure water for preparation of functionalized MoS2 aqueous solutions for further experiments.

7. **Dissociated Mo Species Detections.** A portion of $HAuCl_4$/MoS_2 reaction mixtures was separated and treated with centrifugation at 12000 rpm for 30 min. Subsequently, as-

obtained Au/MoS_2 solids were totally settled down, and the supernatant containing dissociated Mo species was collected for ICP-AES detections. Noticeably, the pure MoS_2 aqueous dispersion without the addition of reacted $[AuCl_4]^-$ was treated with consistent processes, and the result of detected Mo ion concentration was regarded as control.

8. **Table S1**. Zeta-potential values of diverse fractionated MoS_2 samples.

Sample	Z-Average Size (nm)	Zeta-Potential (mV)
(F1) 2k-MoS_2	167.2 ± 3.7	-35.4 ± 1.1
(F2) 4k-MoS_2	150.0 ± 5.6	-34.2 ± 1.7
(F3) 6k-MoS_2	123.9 ± 3.6	-39.9 ± 0.7
(F4) 8k-MoS_2	102.4 ± 4.1	-36.3 ± 1.1
(F5) 10k-MoS_2	89.9 ± 2.3	-33.4 ± 1.7

9. **Figure S1.**

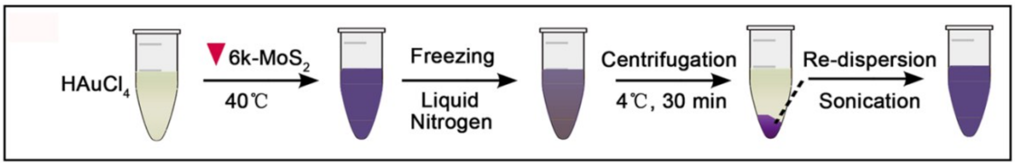

Figure S1. Illustration of freezing processes to collect the time-dependent products of $HAuCl_4$/MoS_2 reactions.

10. Figure S2.

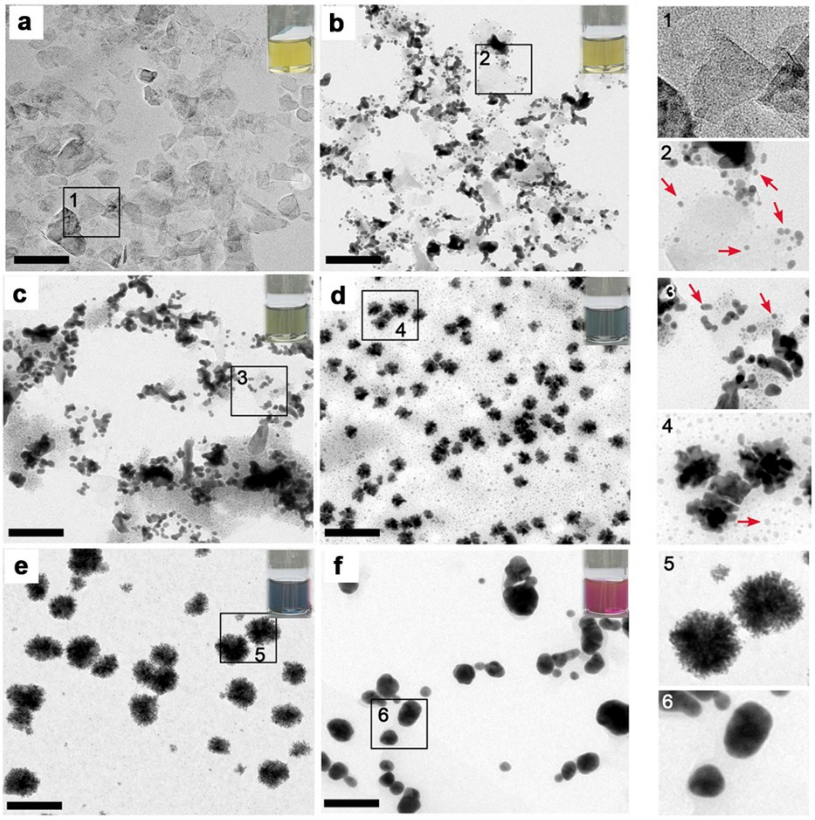

Figure S2. (a-f) TEM images record the morphologies of MoS_2 reacted with $HAuCl_4$ for diverse times after a freezing process. a-f: 0, 1, 3, 5, 8, 15 min. The inset pictures represent the colors of reaction systems after a freezing process. The scale bars in panel a-f are 100 nm.

11. Figure S3.

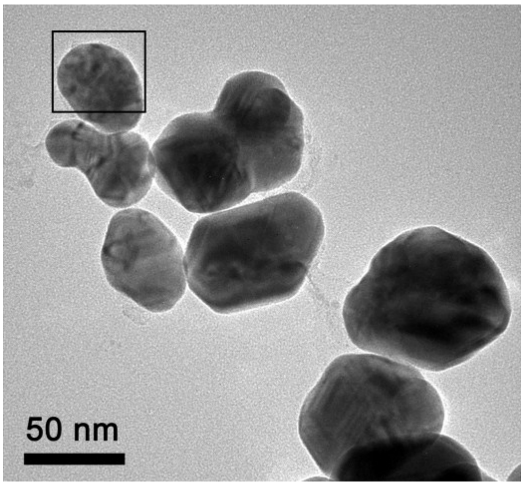

Figure S3. TEM image of Au/6k-MoS_2 reaction products indicating the crystal morphology of nanoparticles.

12. Figure S4.

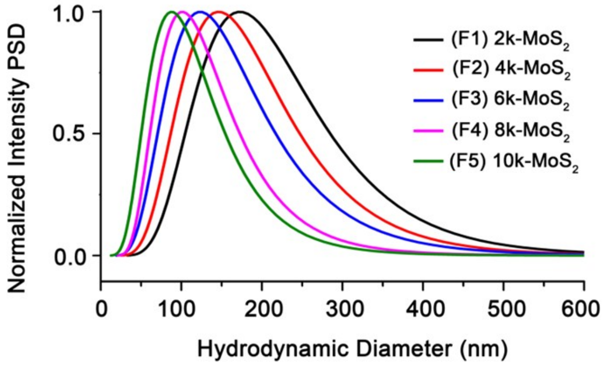

Figure S4. DLS spectra of diverse fractionated MoS_2 samples.

13. Figure S5.

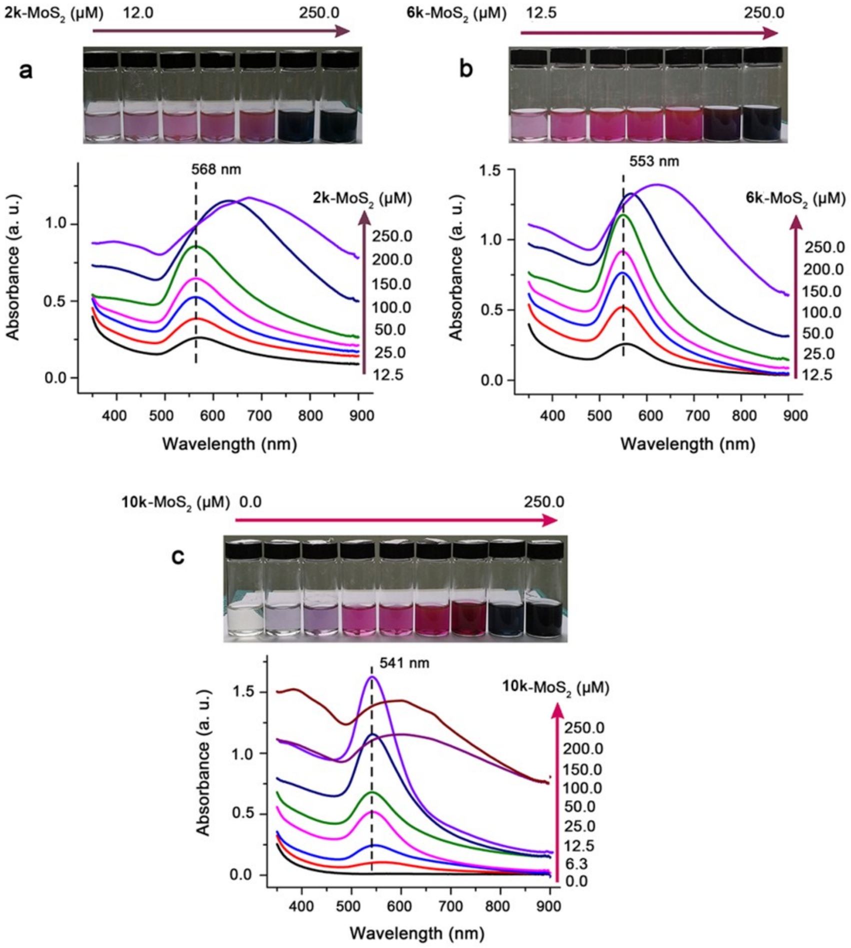

Figure S5. Photonic absorption spectra and corresponding photos of $HAuCl_4/MoS_2$ reaction systems in the presence of various concentrations of fractionated 2k-MoS_2 (F1, a), 6k-MoS_2 (F3, b), and 10k-MoS_2 (F5, c). The concentration of $HAuCl_4$ is 450 μM.

14. Figure S6.

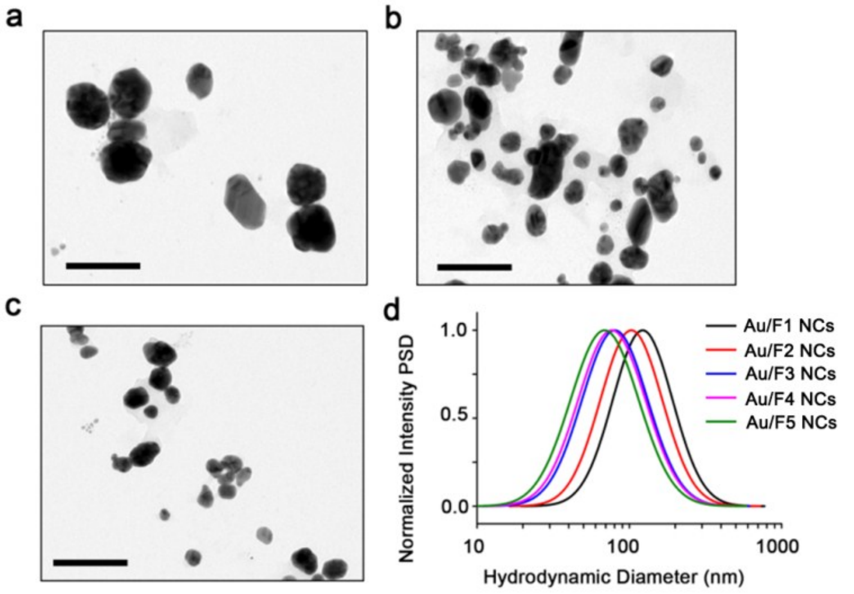

Figure S6. TEM images of (a) Au/F1 NCs, (b) Au/F3 NCs, and (c) Au/F5 NCs. The scale bars in (a-c) are 250 nm. (d) DLS spectra of diverse Au/Fx NCs (x=1, 2, 3, 4, and 5, respectively). The concentration of MoS_2: 150.0 μM; concentration of $HAuCl_4$: 450.0 μM.

15. Figure S7.

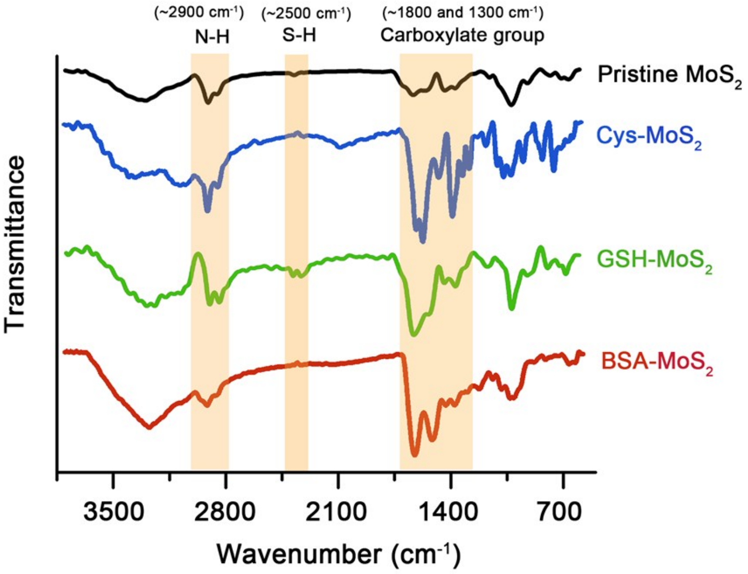

Figure S7. FTIR spectra of diverse MoS_2 samples before and after the incubation with Cys, GSH, and BSA.

16. Figure S8.

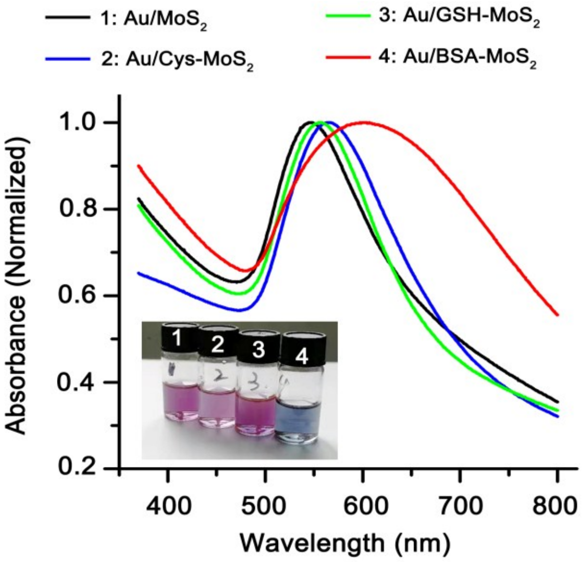

Figure S8. Absorption spectra of diverse Au/MoS$_2$ nanostructures aqueous solutions and their corresponding photos.

17. Figure S9.

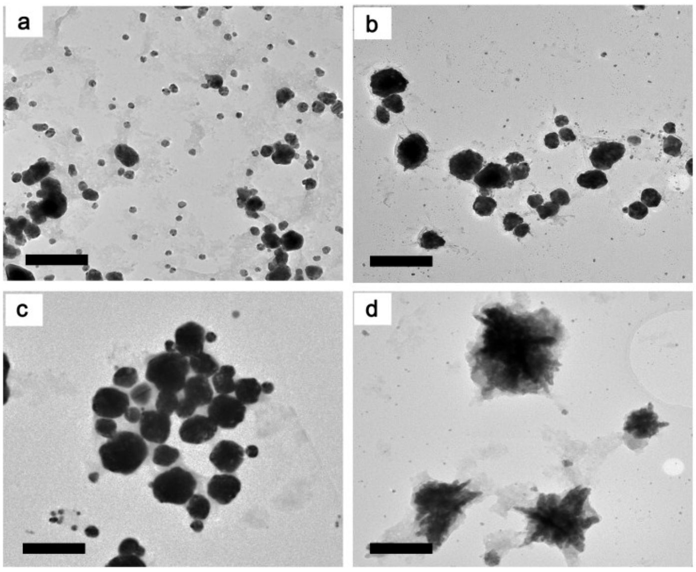

Figure S9. TEM images of reaction products of saturated HAuCl$_4$ and diverse MoS$_2$ samples (a: pristine MoS$_2$, b:Cys-MoS$_2$, c:GSH-MoS$_2$, d: BSA-MoS$_2$). The scale bars are 100 nm.

References

[S1]B. L. Li, H. L. Zou, L. Lu, Y. Yang, J. L. Lei, H. Q. Luo and N. B. Li, *Adv. Funct. Mater.*, 2015, **25**, 3541-3550.

[S2]B. L. Li, M. I. Setyawati, L. Chen, J. Xie, K. Ariga, C. T. Lim, S. Garaj and D. T. Leong, *ACS Appl. Mater. Interfaces*, 2017, **9**, 15286-15296.

[S3]B. L. Li, L. Y. Peng, H. L. Zou, L. J. Li, H. Q. Luo and N. B. Li, *Small*, 2018, **14**, 1703560.

[S4]B. L. Li, H. L. Zou, J. K. Tian, G. Chen, X. H. Wang, H. Duan, X. L. Li, Y. Shi, J. R. Chen, L. J. Li, J. L. Lei, H. Q. Luo and N. B. Li, *Nano Energy*, 2019, **60**, 689-700.

[S5]G. Guan, S. Zhang, S. Liu, Y. Cai, M. Low, C. P. Teng, I. Y. Phang, Y. Cheng, K. L. Duei, B. M. Srinivasan, Y. Zheng, Y. W. Zhang and M. Y. Han, *J. Am. Chem. Soc.*, 2015, **137**, 6152-6155.

[S6]S. C. Chen, C. Y. Lin, T. L. Cheng and W. L. Tseng, *Adv. Funct. Mater.*, 2017, **27**, 1702452.

[S7]Q. Li, Y. Zhao, C. Ling, S. Yuan, Q. Chen and J. Wang, *Angew. Chem. Int. Ed.*, 2017, **56**, 10501-10505.